Design and Patient-Oriented Control of A Rehabilitation Assistance Upper Exoskeleton

Huu-Toan Tran * , **Manh Son Tran** **

* *Faculty of Electronic Technology, Industrial University of Ho Chi Minh City, Ho Chi Minh City, 700000, Vietnam (e-mail: tranhuutoan@iuh.edu.vn)*
** *Automatic Control Department, Ho Chi Minh City University of Technology and Education, Ho Chi Minh City, 700000, Vietnam (e-mail: sontm@hcmute.edu.vn, Corresponding author)*

Abstract: Inspired by the difficulties behind specification requirements as well as realizing the applicable capacity of upper exoskeleton robots, this paper presents the design and development of an original prototype of Rehabilitation Assistance UPper EXoskeleton (RAUPEX). The exoskeleton is designed through the analysis of human's upper limb biomechanics and dynamics. Based on the requirements of human joint power, the solutions of mechanism and actuator for the exoskeleton are drawn. During development of the exoskeleton, a basic control hardware is built to ensure real-time control performance besides a custom-built control panel for users. A patient-oriented control strategy allows RAUPEX to assist patients with various disability level in rehabilitation. The robot's applicable efficiency has been evaluated through rehabilitation training tests on healthy persons as quasi-patients via fundamental criteria in the exoskeleton development. Normalized square sum of angular operator-exoskeleton errors that is $(25.3 \pm 2.45) \times 10^{-3}$ for active control and is $(5.89 \pm 0.42) \times 10^{-3}$ for passive control. Moreover, the resulting operator-exoskeleton interaction force which is maximum of 7.75 N at upper arm and 4.32 N at lower arm enables RAUPEX to accurately assist rehabilitation exercises without discomfort. Over 87% of experimental participants claimed to feel comfortable which proves the developed exoskeleton has the potential to increase efficiency and adaptation to users during rehabilitation procedure.

Keywords: Biomechanics technology; Wearable robot; Upper limb exoskeleton; Rehabilitation robot; Physical human-robot interaction; Control of Exoskeleton.

1. INTRODUCTION

The collaboration between human activities and powered assistive robots is an efficient manner to take full advantage of both human and robot ability. By this way, the robots are able to assist human in difficult and dangerous situations due to their unlimited power from external supplies, such as electric, pneumatic, hydraulic power, or shape memory alloy. As a result, many wearable devices, especially exoskeletal robots, have been developed to bring a numerous practical applications of human assistance in daily life. In particular, for disabled persons or patients with movement difficulties, the forgoing assistive robots play an important role to support them in physical training and rehabilitation (Feys et al. (2019); Fiorini Icon et al. (2019)). According to pathology breakdown that causes severe motor effects and has many sequelae, stroke is thirdly ranked in popularity worldwide (Mackay et al. (2004)). Approximately 30% to 66% of stroke patients did not recover their upper limb function after entering a chronic phase of 6 months. Only 5% to 20% of stroke patients are showed to accomplish the upper limb recovery according to Kwakkel et al. (2003). Therefore, the appropriate therapies to enhance rehabilitation effectiveness for the upper limbs have been proposed, such as standard multidisciplinary rehabilitation with one-to-one manual interactions with therapists (Trulsson Schouenborg et al. (2021)), practice with mirror and imagination (Langhorne et al. (2011)), and robot-aided support (Narayan et al. (2021)). The implementation of functional recovery exercises for patients requires many different procedures depending on the degree and resilience of each patient in each stage (Buma et al. (2013)). Therefore, the service of a large number of patients requires a correspondingly significant staff of therapists and doctors. This is difficult to respond while there are many simple exercises or maneuvers that do not require the direct effort of a therapist but the assistance of "a support machine" for recovery. The exoskeletal robot is a logical solution to this problem, as the robot plays the role as a skeleton-joint system to address and perform movements. Thus the robot is capable of supporting patients in a lot of therapeutic exercises with many different degrees (Mertz (2012); Yeh et al. (2021)). The demand in the development of this robot type has significantly increased due to the increasing trend of stroke as well as

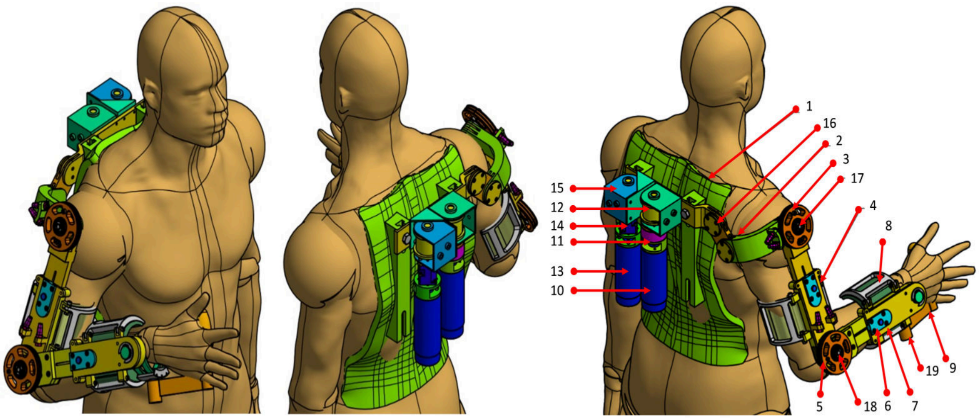

Fig. 1. The RAUPEX design: An exposed views of the Exoskeleton in a reach posture joint angle space. 1. Torso including motors and harmonic drive; 2. Shoulder link; 3. Passive pulley of shoulder; 4. Upper-arm link; 5. Passive pulley of elbow; 6. Adjustable slider cranks; 7. Forearm link; 8. Brackets; 9. Handle; 10. DC motor of shoulder joint; 11. Harmonic drive of shoulder joint; 12. Active pulley of shoulder; 13. DC motor of elbow joint; 14. Harmonic drive of elbow joint; 15. Active pulley of elbow; 16. Passive shoulder joint for adduction/abduction; 17. Actuated shoulder joint; 18. Actuated elbow joint; 19. Passive wrist joint for flexion/extension

spinal cord injured (SCI) patients every year (Virani et al. (2020)).

Rosen *et al.* provided the kinematics and dynamics of human arm model in design of a seven Degree of Freedom (DOFs) (+ 1 hand) powered, redundant, upper-limb robotic system called EXO-UL8 exoskeleton (Sun et al. (2021)). The statistical distribution for human daily actions using the exoskeleton in this research brings meaningful biomechanic fundamentals for upper exoskeleton design. As one of the typical groups in enhance of control quality for the upper exoskeletons, this group developed a multi-level control strategy where the admittance and PD position control loops are simultaneously managed to reduce the resulting interaction force and upper body effort. Unlike traditional stiff control strategies, the proposed strategy computes the joint angles and related force errors to feed to a force/position control law which provides compliant movement characteristics. Thus, the method depends significantly on hardware implementation and a subset of sensors which are necessary to improve for the rehabilitation trials. Similarly, Zimmermann et al. proposed a Hierarchical Optimisation Controller on ANYexo exoskeleton to estimate a subject's voluntary joint torque from a 3-level calculation strategy (Zimmermann et al. (2019)). To perform this control scheme, it was complicated to calculate three priorities using hierarchical optimization. Development of a redundant back-drivable upper limb exoskeleton Armule at the Huazhong University of Science and Technology, He C *et al.* primarily focused on the 5 DOF rehabilitation exoskeletal robot to demonstrate that the exoskeleton has the significant potential to rehabilitation (He et al. (2021)). By proposing a sustainable redundant mechanical design, two electric actuators with cable-driven mechanism, and an embedded control system, the team successfully developed the Armule Robot arm to support rehabilitation and physiotherapy. Wang *et al.* also introduced an exoskeletal robotic system controlled by a predictive human motion intention that assist three DOFs of upper limb in daily activities (Wang et al. (2022)). Although the above researches have successfully acquired the ability to assist human for the rehabilitation exercises, it is still necessary to expand a number of degrees of freedom to support more functionality. Another pioneer laboratory is at Tsukuba University where lightweight powered robotic devices called Hybrid Assist Limbs (HAL) have been developed for multi-function (Hayashi et al. (2005)). HAL electric actuators are controlled at the shoulder, elbow, and wrist joints using an estimate of the operational human intention from Electro-Myo-Graphical (EMG) sensor. HAL and its generations utilized embedded computers as well as intelligent control techniques to not only assist the operator's hand muscles but also support to carry an external load. A prototype of four actuated DOF upper exoskeleton called LIMPACT was introducted by Alexander Otten et al. from Laboratory of Biomechanical Engineering University of Twente using rotational series elastic hydraulic motors (Otten et al. (2015)). The systematical issues consist of kinematics, dynamics and a torque-based impedance control were dealt with as a preamble for the LIMPACT development in future. A 5-DOF lightweight exoskeleton actuated at elbow and wrist joints has been developed for forearm rehabilitation by Wu *et al.* (Wu et al. (2019)). This exoskeleton provides an effective solution for robotic structure due to a novelty mechanism using series elastic actuation and sensing. Similarly to LIMPACT, a two-loop impedance control strategy was also utilized to manage the human-exoskeleton interaction. To reduce the heavy weight of the exoskeleton, a novel 6 DOFs passive upper limb exoskeleton introduced by Vazzoler *et al.* was designed to reach the static balancing using passive elements through the action of ve springs (Vazzoler et al. (2021)). By using a 3R balancer, the robot is able to assist patients in passive rehabilitation exercises in consideration of wearing safety and convenience. A dynamic model-based control proposed by Herbin et al. (Grazi et al. (2020)) minimized the inuence of friction in the closed-loop Bowden cable conduit system. The estimation of the interaction torque with the operator based on the ExoArm 7-DOF exoskeleton dynamics model increases the computation cost for the controller. A novel semi-passive upper-limb exoskeleton system (H-PULSE) was also introduced to reduce the users muscular activity and the heart rate (Grazi et al. (2020)). In this investigation, the exoskeletal structure of active mechanism for regulating the assistance level is concentrated while a conventional two-layer proportional controller was applied. Non-adaptive control and passive constraints in the musculoskeletal design hinder this robot from higher level assistance.

The above typical endeavors are evident that the development of wearable assistive upper exoskeletons is essiential but poses challenges for a numerous applications in rehabilitation (Kapsalyamov et al. (2020); Rehmat et al. (2018)). Due to the human-robot cooperation, it is necessary to consider some key factors in the design of the exoskeletons such as the potential to adapt to different biomechanic individual users; to generate efficient assistive torques/forces; and to minimize the physical human-robot interaction forces/torques besides the safety feature for the robot. Firstly, the exoskeleton is considered to carry the human upper limb during working collaboration, so the anthropomorphic techniques and biomechanical problems need to be dealt with for the exoskeleton design (Zimmermann et al. (2019)). Secondly, the choice of drive source and transmission should be analyzed appropriately to increase performance and reduce weight because the robot is a wearable device (Slucock (2022)). Finally, as a second limb of an operator, the robot's movements should be accurately controlled without discomfort when being carried by various operators with different movement impairments (Herbin et al. (2021); Song et al. (2021)).

From the viewpoint of master/slave motion, the recent control approaches enable the upper exoskeletons only to be master or slave. In other words, the exoskeletons just play the role as robots aimed at operator augmentation (slave) (Grazi et al. (2020); Wang et al. (2022)) or patient assistance (master) (Xie et al. (2021)). For patient assistance, the level of support is also fixed to each patient (Zimmermann et al. (2019); Sun et al. (2021)). This paper proposed a flexible control method called patient-oriented control (POC) that allows RAUPEX to augment human strength and assist human abilities. This control method combine an active mode using state machine control with a passive mode using force-based variable impedance control. This combination allows the robot to support both complete and incomplete motor injury patients. The proposed SOC is evaluated on an exoskeletal robot prototype, called Rehabilitation Assistance UPper Exoskeleton (RAUPEX) designed to support patients in recovery exercises. The remainder of this paper is organized as follows; firstly, the main design results of RAUPEX are briefly introduced. Subsequently, we discuss how hardware and control strategy are implemented on the robot. Finally, experiments will be implemented to evaluate the effectiveness of the robot on recovery exercises in rehabilitation.

2. DESIGN OF REHABILITATION ASSISTANCE UPPER EXOSKELETON

2.1 RAUPEX structure

Based on the analysis of biomechanic data and mechanic solutions, especially the dimensions and limits of the human arm movements (as summarized in Table 1), the computer aided design (CAD) of RAUPEX model on human

Table 1. Kinematic and dynamic parameters for human model and RAUPEX (Max angle (°), Max torque (Nm)). The profile obtained from Winter *et al.* and RAUPEX design specication that was scaled for a 70 kg healthy person's daily activities with load of 5 kg

Joint	Movement	Human model		RAUPEX	
		Max Angle	Max Torque	Max Angle	Max Torque
Shoulder	Extension	-32	-4.5	-30	-44.8
	Flexion	178	10	135	44.8
	Adduction	-15	-1.8	-5	Passive
	Abduction	95	7.5	90	Passive
Elbow	Extension	0	-1.5	0	-32.5
	Flexion	152	2.2	135	32.5
Wrist	Extension	-60	-0.3	-45	Passive
	Flexion	60	0.3	45	Passive

arm is designed using Inventors (AutoDesk Inc.) as shown in Fig.1. The designed model includes five main assembly modules as follows. The torso is the stationary frame that bears all the weight of actuation and mechanisms. This module is worn by operators to create the correlation position so that RAUPEX can assist motor functions on the human arm. The shoulder link is the transitional module from the torso to the shoulder joint, creating a correlation position of the whole limb with respect to the torso. In this link, it is appropriate to allocate a passive degree of freedom for comfortably abduction/abduction movement at the human shoulder. The upper-arm and the forearm (lower) links are the modules that supports the function of the upper-arm and forearm biceps during motion, respectively. The motions of the upper and lower links are provided by two servo motors (Motori Apparecchiature Electtriche M542/080605MPU) through harmonic drives and self-designed cable drive transmissions. The cable tension is tuned by means of a pair of adjustable plugs mounted on the outside of the passive pulleys. The motors are all DC motors attached to encoders, with resolutions of 1000 pulses per revolution. The upper and lower links' length can be adaptive to various users by a self-designed adjustable slider crank mechanism. The handle is the module in which the operator can hold RAUPEX's end effector in hand

2.2 Dynamics of the human-RAUPEX system

The Operator-RAUPEX dynamic model could be drawn to the compact form by derive the Lagrangian dynamics as follows:

$$M(\theta)\ddot{\theta} + C(\theta,\dot{\theta})\dot{\theta} + G(\theta) = \tau - \tau_F - \tau_O, \qquad (1)$$

where $\theta \in \Re^2$ is the generalized angle vector comprising the shoulder and elbow joint angles. The terms $M(\theta) \in \Re^{2\times 2}, C(\theta) \in \Re^2, G(\theta) \in \Re^2$ represent the positive definite inertia matrix, Coriolis and centrifugal torque vector, and gravity torque vector, respectively, of the combined Operator-RAUPEX system. The terms on the right-hand side of Eq. (1) are the torques acting onto the exoskeleton. Of them, τ is the torque vector of linear drives acting onto the links of the exoskeleton, τ_O is the interaction torque vector from the operator to exoskeleton and τ_F is the friction torque vector around the joints of both the exoskeleton and operator.

$$\begin{aligned} M_{11}(\theta) &= m_1 l_{C1}^2 + m_2[l_1^2 + l_{C2}^2 + 2l_1 l_{C2} cos(\theta_2)] + J_1 + J_2 \\ M_{12}(\theta) &= m_2[l_{C2}^2 + l_1 l_{C2} cos(\theta_2)] + J_2 \\ M_{21}(\theta) &= m_2[l_{C2}^2 + l_1 l_{C2} cos(\theta_2)] + J_2 \\ M_{12}(\theta) &= m_2 l_{C2}^2 + J_2 \end{aligned} \quad (2)$$

$$\begin{aligned} C_{11}(\theta,\dot{\theta}) &= -m_2 l_1 l_{C2} sin(\theta_2)\dot{\theta}_2 \\ C_{12}(\theta,\dot{\theta}) &= -m_2 l_1 l_{C2} sin(\theta_2)(\dot{\theta}_1 + \dot{\theta}_2) \\ C_{21}(\theta,\dot{\theta}) &= m_2 l_1 l_{C2} sin(\theta_2)\dot{\theta}_1 \\ C_{22}(\theta,\dot{\theta}) &= 0 \end{aligned} \quad (3)$$

$$\begin{aligned} g_1(\theta) &= [m_1 l_{C1} + m_2 l_1] g sin(\theta_1) + m_2 g l_{C2} sin(\theta_1 + \theta_2) \\ g_2(\theta) &= m_2 g l_{C2} sin(\theta_1 + \theta_2) \end{aligned} \quad (4)$$

where $l_1 = l_{O1} = l_{R1}$ and $l_2 = l_{O2} = l_{R2}$ are lengths of upper arm (link 1) and lower arm (link 2), respectively; Indexes O, R represent for Operator and RAUPEX, respectively; l_{C1}, l_{C2} are distances to the center of mass of upper arm and lower arm; $m_1 = m_{O1} + m_{R1}$ and $m_2 = m_{O2} + m_{R2}$ are masses of upper arm and lower arm of both operator and RAUPEX; $I_1 = I_{O1} + I_{R1}$ and $I_2 = I_{O2} + I_{R2}$ are inertial components relating to center of mass of upper arm and lower arm of both operator and RAUPEX, respectively; g is gravity acceleration

The above dynamic equation is used to test the required power for the actuators and to evaluate a control algorithm as a preamble for the development of the control strategy for the exoskeleton. Moreover, the terms $g_1(\cdot), g_2(\cdot)$ are estimated to compensate for the passive impedance control mode as mentioned in the next subsection 3.3. To check actuator capacity, the parameters of RAUPEX are taken from the design and friction torque τ_F are assumed as functions of joint positions and velocities as follows:

$$\tau_F(\theta,\dot{\theta}) = D_R\dot{\theta} + C_R sign(\dot{\theta}) + D_O(u(t))\dot{\theta}, \quad (5)$$

where D_R, C_R represent viscous friction and Coulomb friction coefficients around the joints of the exoskeleton, respectively; D_O is the viscous friction coefficient around the joints of the operator. In Eq. (5), the stiffness of the operator's muscles is ignored since it is insignificant compared to other parameters. The interaction torque is obtained from the biomechanical data. In addition, a safety factor of 1.45 is added to ensure the power range for the actuator's safety.

2.3 Prototype of RAUPEX

After fabrication and assembly as depicted in Fig. 2, summary of RAUPEX parameters is briefly described in Table 2. These parameters are basically compatible with the design goals, but there are still insignificant geometric errors affected by uncertainties such as eccentricity and assembly deviations. In general, RAUPEX has 4-DOFs in which two actuated DOFs assist the flexion/extension motions at the shoulder and elbow joints and two passive DOFs facilitate the training operation and calibration. The total weight of RAUPEX is 9.25 kg, of which the torso including the harmonic drive and motors weighs approximately 4.0 kg. The range of motion at the shoulder joint is from 135 degree in exion to −30 degree in extension, while the range of motion at the elbow joint is from 135 degree in exion to 0 degree in extension. Shoulder abduction/adduction and wrist abduction/adduction DOFs respectively accommodate the user a range of adjustable angle from −5 to 90 degree and from −45 to 45 degree. Lengths of the forearm

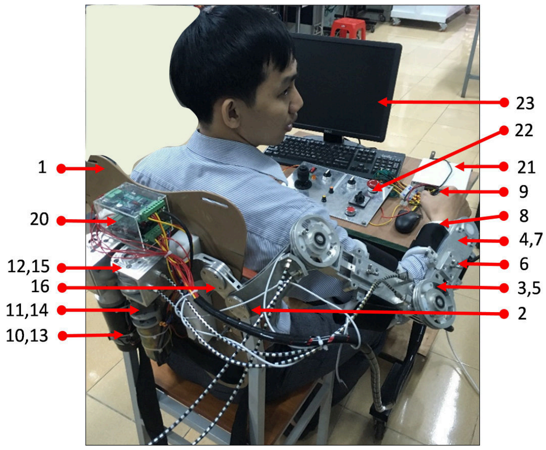

Fig. 2. The RAUPEX prototype: 1 to 19 are the parts corresponding to the RAUPEX design mentioned in Figure 1; 20. Motor drives; 21. PCI card and connector; 22. Control panel; 23. Control PC and monitor

Table 2. RAUPEX specifications after design, fabrication, and testing. In the table, data are obtained from design profile and experimental measurement

	RAUPEX specification
Parameters	Property, value (unit)
Degree of freedom (actuated/passive)	4 (2/2) (DOFs)
Total weight including torso (without torso)	9.25 (5.25) (kg)
Dimention	290x420x820 (mm)
Length (min/max)	470/560 (mm)
Length of upper arm link (min/max)	250/290 (mm)
Length of forearm link (min/max)	220/270 (mm)
Range of motion at shoulder (Flex./Ext.)	-30/135 (°)
Range of motion at shoulder (Abd./Add.)	-5/90 (°)
Range of motion at elbow (Flex./Ext.)	0/135 (°)
Range of motion at wrist (Abd./Add.)	-45/45 (°)
Core material	Aluminum
Electric motor capacity	60 (W)
Max operation frequency (at the joints)	1 (Hz)
Maximum load	5 (kg)

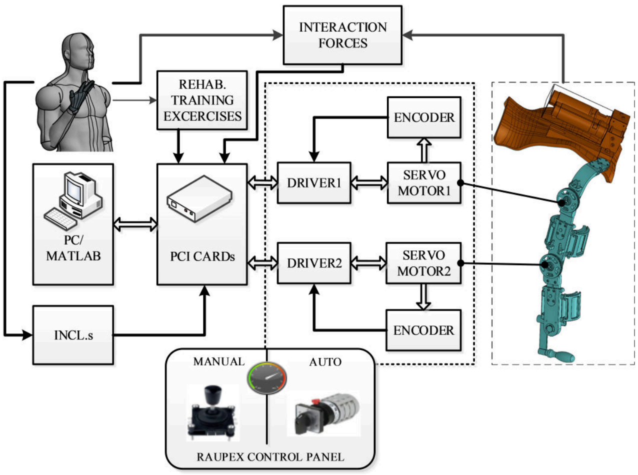

Fig. 3. Hardware diagram implemented on RAUPEX

link and lower arm link can be adjustable from 250 mm to 290 mm, and from 220 mm to 270 mm, respectively. This adjustment ability is enable due to the designed slider cranks at the middle of the links.

According to statistical distribution of peak torques at the shoulder during ADLs reported in the literature, the output of the joint torque about 8 Nm to 10 Nm is sufficient to support rehabilitation exercises without the exoskeleton assistance (Rosen et al. (2005)). The motor is a Motori rotating brushless DC motor with a power rating of 60 W, a continuous torque rating of 0.64 Nm. The transmission ratio of the harmonic drive is 40 : 1 resulting in an output torque of 25.6 Nm. The ratio of cable-pulley transmission is 1.75 thus the final output torque is 44.8 Nm in the above permitted range. This power calculation has been reevaluated using dynamic model of the human-exoskeleton system including the assumption of the physical interaction and the friction torque in Eq. (1).

3. EXOSKELETON CONTROL

3.1 Hardware configuration

RAUPEX is a biomedical robot system interacting with users, so the control system design is required to meet safety criteria including safety source and safety interrupt, and to meet the human-machine interface in addition to the requirements of real-time precise control. The control hardware of RAUPEX is implemented as shown in Fig. 3. The computer plays a central control role using Matlab RealTimeWorkshop application. Two PCI 6221 NI (National Instrument) cards facilitate the real-time control and communicate to the computer via computer's PCI Express slots to provide a consistent behavior and comfortable data visualization. Two digital servo drives (Modular Servo Drive-MSD) capable of delivering about 20 A of continuous current are fed to drive the DC motors. The custom-built control panel and the corresponding human-machine interface are additionally built to select pre-programmed control modes and training exercises for users. In order to measure joint angles of the both operator's upper limb and exoskeleton's links, encoders on RAUPEX's drives and inclinometers on the operator's limbs are used. Two integrated optical incremental encoders with a resolution of

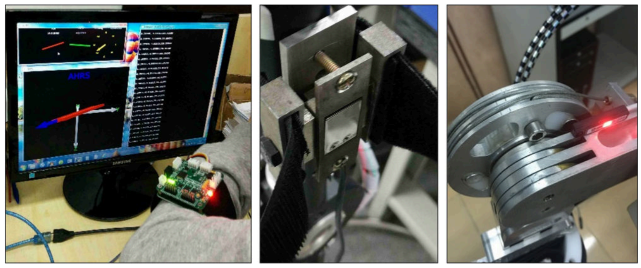

(a) (b) (c)

Fig. 4. Testing inclinometer on 3-D model (a), two-dimensional interaction force sensors (TIFSs) (b), and limit sensor at a safety range (c)

1000 pulses per revolution are attached to the motors shaft for the measurement of the exoskeleton's joint angles. Two custom-built inclinometers are attached to the operators upper arm and forearm to measure the angular positions relative to the gravity. The inclinometer is built using a MPU-6500 six-axis motion tracking sensor that combines a 3-axis gyroscope and a 3-axis accelerometer in a package and provides high resolution measurement. A low-cost micro control unit (STM32F405, 32 bit, 168 MHz frequency) is used to capture the inclination data stream and to implement Kalman filtering. The performance verification for one of the designed inclinometers is displayed on a 3-D demo as shown in Fig.4a. The quasi-interaction forces resulting from human arm on the RAUPEX are measured by custom-built two-dimensional interaction force sensors (TIFSs) as shown in Fig.4b. The TIFSs are integrated into the human-exoskeleton connection belts through upper arm and forearm cuffs can measure the flexion/extension deformation of the belt forced by the operator's limb. Additional details of the inclinometers and TIFSs can be found in our previous study (Tran et al. (2016)). It is worth noting that the TIFSs signal is not completely the entire force exerted by the operator on the RAUPEX but is utilized to obtain the representative change in the interaction force. In the scope of patient-oriented control as mentioned later, this signal is accounted for constructing the trigger threshold and also the desired impedance between the operator and RAUPEX. Additionally, four magnetic sensor switches are selected to detect the motion limit of the robot at the shoulder and elbow joints and to reset the system to the zero position as shown in Fig.4c. These sensors also ensure the safety of the RAUPEX operation at the second safe mode.

3.2 Human-machine interface and safety modes

A control panel and a human-robot interface (HRI) on Matlab Guide are provided to facilitate users and collect assessment data. On the interfaces, there are functions of manual and patient-oriented control. Especially, the HRI is designed corresponding to control strategy of RAUPEX, thus it allows a therapist to set up control parameters, e.g, impedance coefficients. The control panel is custom-built design so that users can actively control RAUPEX in manual mode or automatic mode instructed by the therapist. Additionally, the panel consists of a number of function keys and an emergency button. As mentioned above, the RAUPEX robot system is aimed to serve patients, so the safety feature is considered priority. Three-layer safety rule is proposed: safety in mechanical structure

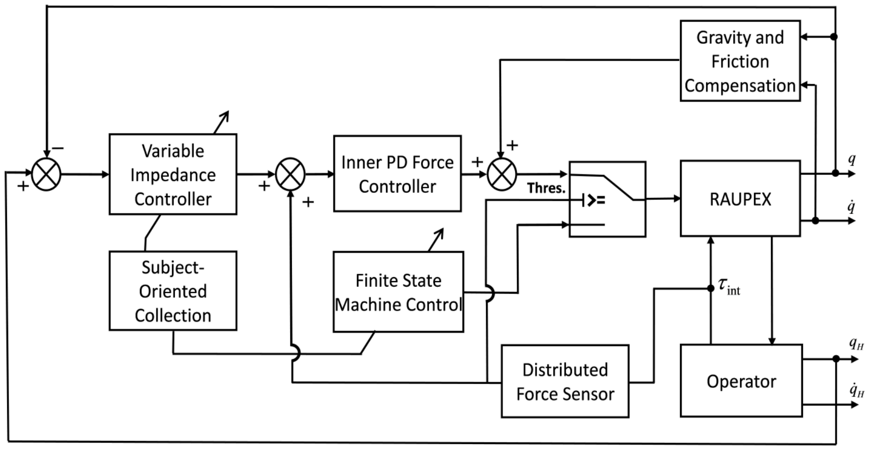

Fig. 5. Principle of the patient-oriented control for RAUPEX interacting with operator. The quasi-interaction force is measured by distributed force sensor (block) using strain gauge integrated into the human-exoskeleton connection. This sensor is not explicitly the entire force exerted on RAUPEX but to obtain the corresponding change in the interaction force for the calculation of the impedance control output and the trigger threshold. Two main controllers are finite state machine control (block) and variable impedance control (block) which are chosen by Patient-oriented selection (block) on the interface. The impedance control calculates the desired impedance compared with the quasi-interaction force for the inner PD force controller (block). To calculate control output of the variable impedance control, a gravity and friction compensation (block) is added to enhance the effective control

(1); safety in electric power by emergency signal (2); safety in control interrupts (3). First, in mechanical design, two slider mechanisms for blocking the movement limitations of joint angles are placed along the shoulder and the elbow joints to ensure that the rotation angles do not exceed the defined motion limit. Table 2 shows the motion limits at these joints in accordance with the designed mechanical structure. Whether the actuators have been a problem or the electric power has not been disconnected, this safety layer ensures that RAUPEX does not compromise the user. Second, as a conventional automatic machine, an emergency stop mode is designed in the power circuit to prevent control problems. Third, in the control loops of manual and automatic modes, the controller is set to reboot using a parallel interruption loop whenever the tracking angle error is over 10 degrees. This interruption loop is also activated when the time response is not obtained within the allowed time period. In addition, there is another soft interrupting mode to limit a peak torque on the servo motor driver when the maximum current for this drive is initially set up.

3.3 Patient-oriented control

Rehabilitation exercises are basically a process of repetitive joint movements. Due to impaired limb function of patients, a therapist is assigned to assist the patients for the training exercises. Depending on the level of impaired limb function, rehabilitation training exercises are significantly assigned for each patient. From the viewpoint of exoskeleton control, the patients (called operators) are classified into two groups: complete and incomplete motor injury patients. For the complete motor injury patients, active control mode should be utilized. In this case, state machine control is applied for RAUPEX in which predefined trajectories were collected from rehabilitation training exercises. For the incomplete motor injury patients, a passive control mode will facilitate the operator-exoskeleton system to be

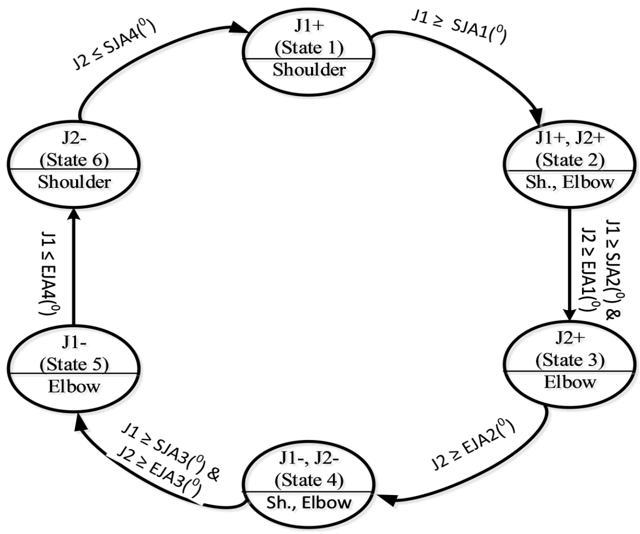

Fig. 6. Finite-state machine control for one of the exercises programmed for RAUPEX ($Exercise_{31}$). In the figure, the abbreviations J1- Shoulder Joint; J2- Elbow Joint; SJA- Shoulder Joint Angle; EJA-Elbow Joint Angle are used

a master-slave system. Impedance control is an appropriate choice for this mode since this control approach allows the exoskeleton to interact dynamically with its environment, i.e., the operators interaction (Lee et al. (2018)). Moreover, this interaction changes from person to person and also within one person over time thus a force-based variable impedance control, as implemented in our previous study, will be used to drive the achieved solution for RAUPEX (Tran et al. (2016)). Considering the above situations arising from using demand and control performance, we proposed a patient-oriented control (POC) strategy which is divided into two main modes corresponding to two kind of patients: a finite-state machine control of active mode for complete motor injury subjects and a variable impedance control of passive mode for incomplete motor injury subjects. The active mode aims to assist fixed training exercises while the passive mode approach to supply as much effort as a patient need to perform exercises. The average value of the distributed forces is compared to a pre-defined threshold to determine which control mode is being stated. In each control mode, the related parameters of each control mode are selected properly, called patient-oriented collection. For example, impedance parameters of the impedance control or training exercise of finite-state machine control are assigned by therapist. Fig.5 shows a detail of the POC strategy describing how the control modes could be triggered and implemented for RAUPEX.

Finite-State Machine Control For a typical training exercise, the trajectories of the shoulder and elbow joints are incorporated together according to the exercise assigned by a therapist. In this training exercise, flexion/extension movements are performed at the shoulder and elbow joints while the transitions are triggered by limit points on the desired trajectories. Based on this principle, finite-state machine control technique is applied to the exercise named $Exercise_{ij}$ (Ex_{ij}) in the control panel where i is level of complexity and j is level of movement velocity. These exercises are predefined and updated corresponding to recovery progress of each individual patient. Fig.6 shows the finite-state machine control model of $Exercise_{13}$ for programming as an example. Assisted upper arm shift to up (State 1) and assisted lower arm shift to up (State 3) are dened for the active control of single joints, of which the signal collected from the position encoder is to lock transition conditions. State 2 and State 4 are dened for the training of the both joints simultaneously until the joints return to the initial (zero) positions of RAUPEX (State 5 and State 6).

Impedance control As mentioned in our previous study, the force-based impedance control is one of the efficient methods for the exoskeleton systems on both upper and lower limbs (Tran et al. (2016); Lee et al. (2018)). This is because the control method seeks to realize a specific impedance between the upper exoskeleton robot and its environment, i.e., the operators hand, rather than enforcing strict pre-defined exercises upon the robot (Zeng et al. (1997); Chiaverini et al. (1999)). From the viewpoint of impedance/admittance approaches, position-based impedance control is commonly applied for robotic systems interacting with high stiffness environments while force-based impedance control is more suitable for the exoskeleton systems interacting with biomechanic environments significantly affected by inertial element (Tran et al. (2014)). As a result, the force-based impedance control method is adopted for the passive control mode in this study. The issues of the stability boundaries of the impedance control system for robots interacting with environments have been proved by Hogan (Hogan (1985)), then the impedance control performance of the passive mode will be principally validated in this paper. In the RAUPEX-operator system, the relationship between the desired impedance torque and the deviation between the joint angles of the operator and robot is considered as a general impedance model describing as follows:

$$\frac{\tau_{Ik}(s)}{\Delta\theta_k(s)} = J_k s^2 + D_k s + K_k, \tag{6}$$

where, J_k, D_k and K_k are the inertial, damping, and stiffness coefficients at shoulder joint ($k = 1$) and elbow joint ($k = 2$), respectively. The term $\Delta\theta_k(s) = \theta_{Ok}(s) - \theta_{Rk}(s)$ is the joint angular deviation between the operator (stands by O) and RAUPEX (stands by R) joint angles. The characteristics of the operator-RAUPEX interaction across different levels of training exercises and movement speeds needs a supervised adjustment of the impedance parameters by a therapist.

As illustrated in Fig.5, the passive impedance control mode is triggered by a pre-defined threshold of interaction torque based on the detected interaction force on the belt of the exoskeleton. As discussed in the subsection 3.1, the custom-built TIFSs estimate the physical interaction forces f_O resulting from the operator to HUALEX at the connections on upper arm and forearm. Although the resulting interaction forces are not straightforward to estimate, it is assumed that these forces are significantly concentrated at the connections. The output joint torque τ of RAUPEX equals the sum of an inner PD controlled torque and a compensation of gravity and friction. The impedance parameters (J_k, D_k, K_k) are updated on the HRI system by the therapist before every exercise. The deviation $\Delta\theta_k$ of the operator joint angle θ_{Ok} and RAUPEX joint angles θ_{Rk} as well as its derivative are utilized to calculate the impedance moment $\tau_{I,k}$. In the proposed control strategy, the encoders attached on the RAUPEX drives measure the exoskeleton joint angles θ_{Rk} at the shoulder and elbow joints, while the inclinometers attached on the operators upper arm and forearm detect the corresponding operators joint angles, θ_{Ok}.

4. EXPERIMENTAL RESULTS AND DISCUSSION

4.1 Experimental procedure and evaluation criteria

For primary evaluation of RAUPEX, experiments were independently conducted with four selected heathy operators whose weights were 72 kg (operator A), 62 kg (operator B), 68.5 kg (operator C), 74 kg (operator D). Each operator was instructed by a therapist to wear RAUPEX and to perform the repetition of a training exercise that could be selected and displayed on the monitor. Three of the repetition were recorded randomly to validate control performance. In order to set up experimental platform, the operators wore the exoskeleton at the upper arm and forearm brackets, and fixed the inclinometers properly at their arms simultaneously. For the both control modes of the proposed patient-oriented control strategies, it is efficient to define performance indexes of quantitative compliance, AE and IF, are as follows:

$$AE_k = \frac{\int_0^{T_c} e_k^2(t)dt}{\int_0^{T_c} \theta_{Ok}^2(t)dt}; \qquad IF_k = \frac{\int_0^{T_c} f_{Ok}^2(t)dt}{\int_0^{T_c} \theta_{Ok}^2(t)dt}, \tag{7}$$

where $AE_k(k = 1, 2)$ is the normalized square sum of angular errors (e_k) at the shoulder joint (AE_1) and the elbow joint (AE_2) in the interval T_c. Also, $IF_k(k = 1, 2)$ is the normalized square sum of the interaction forces (f_{Ok}) at the upper arm cuff (IF_1) and the forearm cuff

Table 3. Semantic Differential Evaluation (SDE) of the operators feeling

SDE	Mark				
	-2	-1	0	1	2
Operationality	obstructed	slightly obstructed	–	slightly comfortable	comfortable
Stress level	heavy	slightly heavy	–	slightly light	light

(IF_2). After every experiment, the operator's feeling of the support ability from RAUPEX were collected besides the foregoing performance indexes. As described in Table 3, the feeling of operationality with RAUPEX was dened as the comfort level of whether an operator could operate his/her hand according to initial intention or not. This Semantic Differential (SD) evaluation approach is advocated for the subjective evaluation of the exoskeleton systems (Lee et al. (2005)).

Tuning process of the inertial, damping, and stiffness coefficients for impedance control mode was experimentally conducted by the therapist. This process was accomplished based on the operator's feeling from the RAUPEX support. Considering the stiffness coefficient, for example, if the operator felt a significant discomfort, this coefficient would be tuned to decline gradually. According to our previous studies, over a normal velocity range of exoskeletons interacting with human, the damping coefficient affects on control quality significantly larger and more irregular than the inertial and stiffness coefficients (Tran et al. (2014)). Therefore, the inertial and stiffness coefficients were first fixed in range of [0.05 0.25] $kg.m^2$ and of [20 40] Nm/rad, respectively, corresponding to each joint and each exercise. This facilitates the job of the therapist to tune the viscous coefficient gradually. The mapping between the level of impaired limb function of a patient and the tuned viscous coefficient was collected before this coefficient was set for every training session. The experiments were individually performed in two modes of the patient-oriented control: (i) the passive finite-state machine control for quasi-disabled patients and (ii) the active impedance control for the assumed incomplete injury motor patients. For primarily evaluation of finite-state machine control mode, we defined five different training exercises and three levels of training speed. Each exercise have the joint trajectory designed according to functional recovery program for various discovery levels. For impedance control, the patients performed randomly training exercises whose trajectories are similar to sinusoid waveforms. Experimental results were evaluated through the mentioned criteria.

4.2 Active mode

In order to confirm the ability of RAUPEX to operate stably and safely, we first conducted swing exercises at each joint in which speed varies from $\pi/4$ [rad/s] to $3\pi/2$ [rad/s]. This range is divided into three speed levels for the finite-state machine control algorithm. The swing exercises were also utilized to check workspace of the shoulder and elbow joint angles. For performance evaluation of the finite-state machine control mode, five predefined exercises were implemented at the three training speeds. Each exercise was repeated three times in which data was collected and averaged to evaluate. As mentioned above, the collected data are the joint angles of both the operator and exoskeleton, and the resulting interaction forces at the upper and lower cuffs through each session.

Fig.7 and Fig.8 show the control performances of one of the training exercises, namely, $Exercise_{31}$ at the shoulder and elbow joints, respectively. As mentioned in section 3.3, $Exercise_{31}$ means the level of complexity is 3 and the level of movement velocity is 1 ($\pi/4$ rad/s). It can be seen that angular operator-RAUPEX tracking errors with the finite-state machine control are asymptotic to zero at every triggered set point of the predefined trajectory. Quantitatively, the normalized square sum of angular errors for the both joints slightly increases corresponding to higher training speeds. For instance, as summarized in Table 3, the average tracking error of the shoulder joint at the speed of $\pi/4$ [rad/s] is increased by 2.5% and 4% of that at the speeds of $5\pi/8$ [rad/s] and $3\pi/2$ [rad/s], respectively. Besides, there is a slight overshoot whose maximum percent value is around 2% to 5% at the both joints at all speeds indicating relative stability of the system. The resulting interaction force at the upper arm is regular from -0.45N to 0.45N except transition moments. For example, when the state of the upper arm shifts from 30 degree to 90 degree, the interaction force reaches a peak value of 7.75 N then reduces to approximately 0.40 N. This means the interaction force is significantly resulted at the moment of transition while RAUPEX does not impede the operator's motion during stable state. The peak value of the interaction force at the upper arm is increased by about 13.6% compared that at the lower arm. Table 4 shows the performance indexes AE and IF with respect to different training exercises and operators at the three levels of training speed. Besides, the operators feeling through three iterations of each exercise are summarized in this table. In general, the normalized square sum of angular errors AE is less than 30.6×10^{-3} at the shoulder and less than 49.2×10^{-3} at the elbow joint. The changes in AE at the both joints are regular since AE_k increases insignificantly according to levels of speed and complexity of each exercise. For example, the operator-RAUPEX control performance at shoulder gives rise to the

Table 4. Experimental results of active mode control on four operators (A-D): Mean values of AE and IF for the operator-exoskeleton control performance across different training exercises and training speeds ($Exercise_{ij}$); and evaluation of the operator's feeling recorded in the first and third sessions for every exercise

No.	Description (sex, weight, height)	Arm length (l_1/l_2 mm)	Exercise (Ex_{ij})	Performance indexes at shoulder		Performance indexes at elbow		(SDE) of the operators feeling	
				AE_1	$IF_1(10^{-3})$	AE_2	$IF_2(10^{-3})$	First session	Third session
	Operator A		Ex_{32}	0.0229	6.81	0.0432	3.18	1	1
1	(man, 72 kg,	292/240	Ex_{22}	0.0243	6.72	0.0441	2.92	1	2
	1.70 m)		Ex_{13}	0.0235	6.94	0.0458	3.02	2	1
	Operator B		Ex_{12}	0.0212	6.32	0.0397	2.83	2	2
2	(woman, 62 kg,	272/220	Ex_{31}	0.0205	6.17	0.0411	2.75	2	2
	1.61 m)		Ex_{41}	0.0201	6.08	0.0426	3.06	1	2
	Operator C		Ex_{23}	0.0219	6.46	0.0407	3.11	2	1
3	(man, 68.5 kg,	285/231	Ex_{41}	0.0238	6.58	0.0415	3.15	1	1
	1.66 m)		Ex_{33}	0.0225	6.71	0.0426	2.89	2	1
	Operator D		Ex_{41}	0.0259	6.92	0.0481	3.21	1	1
4	(man, 74 kg,	308/255	Ex_{53}	0.0306	7.16	0.0492	3.42	-1	1
	1.72 m)		Ex_{32}	0.0272	6.75	0.0466	3.04	1	2

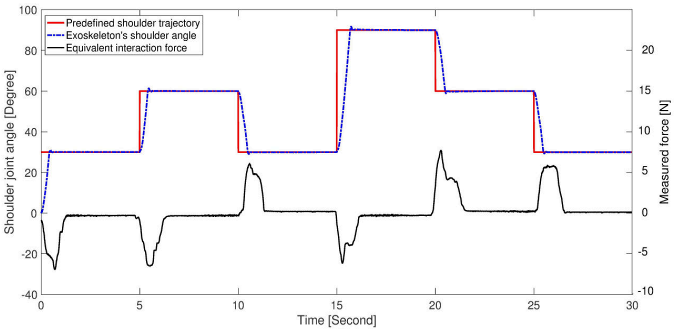

Fig. 7. Control performances at shoulder joint of the active finite-state machine control with $Exercise_{31}$

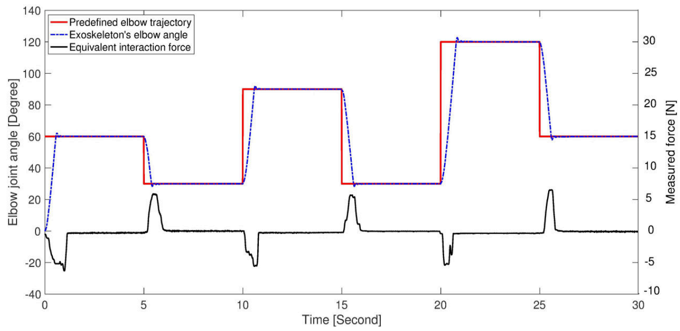

Fig. 8. Control performances at elbow joint of the active finite-state machine control with $Exercise_{31}$

maximum AE of 30.6×10^{-3} for operator D in experiment Ex_{53} and to the minimum AE of 20.1×10^{-3} for operator B in experiment Ex_{41}. Even though the trajectories are different from each joint and from each training exercise, the changes in the index AE show a stable tracking error range in the active control mode. This ensures that the human-exoskeleton system has been operated within a permissible range safely.

The average amount of interaction force tends to increase slightly with the increase of the complexity level of the training exercises. Specifically, IF_1 for operator D increases approximate 18% compared to IF_1 for operator B whose musculoskeletal moment is lower corresponding to his biomechanic properties, *i.e.* his weight and height. The interaction at shoulder gives rise to maximum IF of 7.16×10^{-3} for operator D in experiment Ex_{53}. The resulting interaction force of the same exercise at the lower arm is also decreased by from 2.18 to 2.56 times compared that at the upper arm. This is understandable since human torque at the shoulder is significantly higher than that at the elbow in biomechanics analysis of ADLs. There are no any extraordinary changes in the resulting interaction force through all the training exercises. This enables us to confirm that RAUPEX in the active mode has the ability to assist various individual users with sufficient accuracy. For each operator, the mark of SDE in all sessions is from 1 to 2 except the case of operator D with exercise Ex_{53}. Of them, operator B with exercises Ex_{1j} to Ex_{3j} feels "comfortable" since these exercises contain simpler trajectories than others. Only two of thirty-six times of the experimental sessions induce that the operators feel slightly obstructed while none of them feel sufficiently obstructed. The Semantic Differential (SD) evaluation provides that approximately 94.4% of the operators feeling are quite comfortable and higher. Furthermore, the equivalent resulting interaction torques, as discussed above, are from 12% to 16% of musculoskeletal moments of human arm

Table 5. Experimental results of passive mode control on four heathy operators (A-D): Mean values of AE and IF for the operator-exoskeleton control performance across random training exercises; evaluation of the operator's feeling recorded in the first and third sessions for every exercise

No.	Description (sex, weight, height)	Arm length (l_1/l_2 mm)	Number of sessions	Performance indexes at shoulder		Performance indexes at elbow		(SDE) of the operators feeling	
				AE_1 (10^{-3})	IF_1 (10^{-3})	AE_2 (10^{-3})	IF_2 (10^{-3})	Third session	Fifth session
1	Operator A (man, 72 kg, 1.70 m)	292/240	6	5.921	9.632	4.720	9.169	1	2
2	Operator B (woman, 62 kg, 1.61 m)	272/220	6	5.667	9.241	4.513	8.924	2	2
3	Operator C (man, 68,5 kg, 1.66 m)	285/231	6	5.752	9.458	4.701	9.127	2	1
4	Operator D (man, 74 kg, 1.72 m)	308/255	6	6.132	10.202	4.945	9.352	1	1

that insignificantly affects to the assisted movements. It means that RAUPEX in the active mode could assist the operators with comfort in various conditions of training exercises, speeds, and subjects.

4.3 Passive mode

In order to evaluate the passive impedance control mode, each operator was instructed to perform six similar repetitions of a random training exercise. Fig.9 and Fig.10 show the control performances of a random training exercise in which operator B generates active torque of a quasi-patient for command signal. It can be seen that angular operator-RAUPEX tracking errors with the active impedance control are also asymptotic to zero over the random trajectory. Similar to the active mode, the normalized square sum of angular errors are also increased corresponding to higher training speeds, yet not significant. For example, as summarized in Table 5 the average tracking error of the shoulder joint at the lower speed approximated 1.2 [rad/s] is increased by 7.5% of that at higher speed approximated 2.0 [rad/s]. The resulting interaction force is regular from −4.32 N to 4.75 N at the upper arm and from −4.11 N to 4.53 N at the lower arm. The peak value of the interaction force at the upper arm is increased by about 12% compared to that at the lower arm. In all the training sessions, there are no any extraordinary change in the resulting interaction force. For example, as seen in Fig.9, when the state of the upper arm transists from a peak shoulder angle of 135 degree, interaction force correspondingly reaches a peak value of −4.32 N then trends to decline gradually corresponding to the reduction of the shoulder angle. This means the interaction force is regularly resulted while RAUPEX assists the human arm yet does not impede the operators motion.

Table 5 shows changes in AE and IF with respect to different random training exercises for each operator. These

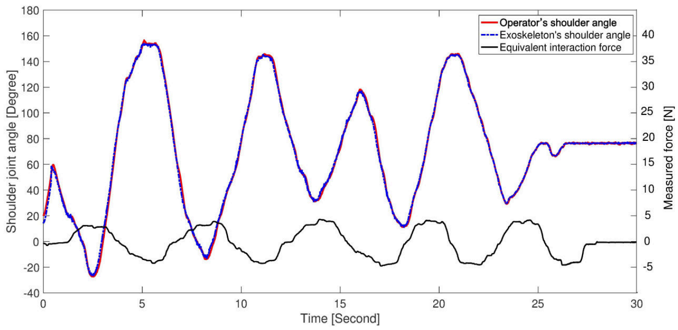

Fig. 9. Control performances at shoulder joint of the passive impedance control with a random trajectory

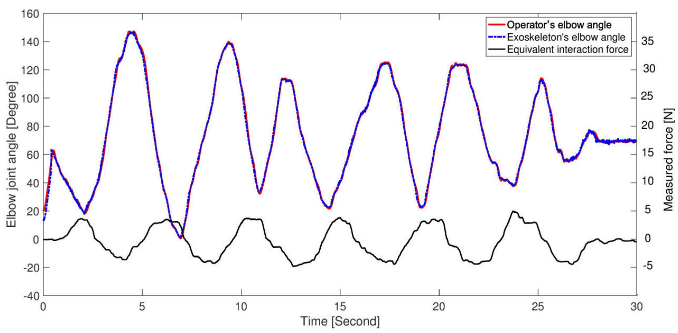

Fig. 10. Control performances at elbow joint of the passive impedance control with a random trajectory

exercises are able to vary for every iteration due to the operators intention. The operator-RAUPEX control performance at the shoulder gives rise to maximum AE of 6.132×10^{-3} for operator D and minimum AE of 5.667×10^{-3} for operator B. In all sessions, the maximum deviation of AE is about 8.2% at the shoulder joint and about 9.5% at the elbow joint. These deviations can be explained due to individual differences among operators as well as among intended motions. Similarly, the maximum deviation of IF is about 10.4% at the upper arm and about 4.7% at the lower arm. Even though the intention-based trajectories are different from each joint and from each training exercise, the changes in the index IF shows a stable interaction range of about 8.9×10^{-3} to 10.2×10^{-3}. This can be explained by the fact that the active torque from the exoskeleton is controlled in operation range, and there are no sudden forces resulting from the physical interaction between RAUPEX and the operators. For the passive mode control, the mark of feeling in all experiments is from 1 to 2 in which operator B feels "comfortable" in all sessions. Only three of twenty four experimental sessions induce that the operators feel fairly obstructed while none of them feel significantly obstructed. The proposed POC strategy in passive mode achieved substantial support that led to approximately 87.5% of the operators feeling are slightly comfortable and higher. Besides, the equivalent resulting interaction torques, as represented in Fig.9 and Fig.10 are from 15% to 18% of musculoskeletal moments of human arm that is input to the impedance adjustment yet do not impede the assisted movements.

5. CONCLUSION AND FUTURE WORKS

This paper puts forward the design and control of a rehabilitation assistance upper exoskeleton, called RAUPEX, capable of supporting human arm muscle. Here, the essential issues related to a prototype of the exoskeleton consisting of the analysis of human upper limb biomechanics, the solution of mechanism, the human-machine interface, and the safety modes have been presented as a preamble for the development of the exoskeleton. In particular, a new patient-oriented control (POC) strategy of the exoskeleton based on the combination of an active finite-state machine control for disabled persons and a passive impedance control for incomplete motor injury patients has been proposed and implemented on a custom-built realtime hardware.

To evaluate the proposed POC on RAUPEX prototype, experimental platforms were implemented to test the both control modes corresponding to the two kind of patients: 1) For active mode, the operators wore the exoskeleton to execute the predefined exercises which classified into five different training exercises and three levels of training speed 2) For passive mode, the operators wore the exoskeleton to perform random training sessions to evaluate the functionality of the exoskeleton compared to the active mode. Even though the subjects, the exercises, and the training speeds are various in the experimental sessions, the changes in the normalized square sum of angular errors and interaction forces showed a stable operator-robot tracking in the both active and passive control modes. The control performance as well as Semantic Differential (SD) evaluation indicated that the exoskeleton can provide assistive torques to human muscle with different physical condition at any speed within a pre-specified range. However, the normalized square sum of angular errors and interaction forces had a tendency to increase gradually along with training speed and operators athletic. This demonstrated that the impact of inertial, friction and manufacturing error of the prototype on control performance at a higher operation frequency range. The job of a therapist will be significantly reduced with the assistance of robot. Instead of conducting a patient for all training steps from person to person, the therapists only set up initial conditions of the training process such as guiding to wear the robot, selecting training exercises and tuning impedance parameters. Future work is to improve RAUPEX structure and material such that the exoskeleton can be carried more convenience. The POC control performance is limited in operation range of $\pi/4$ rad/s to $3\pi/2$ rad/s. It should be enhanced to a wider range of $3\pi/2$ rad/s to $2\pi/$ rad/s by changing driver hardware and then reducing control sampling time. Another solution to enhance the operation range is to change material of RAUPEX from aluminum to hybrid composite or titan because current weight of the robot is relatively high (over 9 kg). Parameters of the passive impedance control such as damping, and stiffness cofficients should be optimized based on data collected from control performances using enhanced genetic algorithms or meta-heuristic optimization algorithms.

ACKNOWLEDGEMENTS

The authors would like to express our sincere appreciation to Thanh-Duy Nguyen at University of Medicine and Pharmacy, Ho Chi Minh City for his contribution on the human biomechanical data collection and to Hoang-Vu Nguyen, Chanh-Tin Nguyen, Ha-Nghiem-Trang Huynh at Faculty of Mechanical Engineering, Ho Chi Minh City Industry and Trade College, for their contribution on the RAUPEX manufacturing.

REFERENCES

Feys P and Straudi S (2019), Beyond therapists: Technology-aided physical MS rehabilitation delivery, *Multiple Sclerosis Journal*, **25**(10):1387-1393

Fiorini Icon L, De Mul M, Fabbricotti I, et al. (2019) Assistive robots to improve the independent living of older persons: results from a needs study, *Disability And Rehabilitation: Assistive Technology*, **16**:92-102

Mackay J, Mensah G, Mendis S, et al. (2004), The Atlas of Heart Disease and Stroke, *World Health Organization.*

Kwakkel G, Kollen BJ; van der Grond J, *et al.* (2003), Probability of Regaining Dexterity in the Flaccid Upper Limb, *Stroke*, **34**(9): 2181-2186.

Trulsson Schouenborg A, Rivano Fischer M, Bondesson E et al. (2021) Physiotherapist-led rehabilitation for patients with chronic musculoskeletal pain: interventions and promising long-term outcomes, BMC Musculoskelet Disord 22 (910)

Langhorne P, Bernhardt J, Kwakkel G (2011), Stroke rehabilitation, *The Lancet*, **377**(9778):1693-1702.

Narayan J, Kalita B and Kumar Dwivedy S (2021), Development of Robot-Based Upper Limb Devices for Rehabilitation Purposes: a Systematic Review, *Augmented Human Research*, **6**(4)

Buma, F, Kwakkel G, Ramsey N (2013), Understanding Upper Limb Recovery after Stroke, *Restorative Neurology and Neuroscience*, **31**(6):707-722.

Mertz L (2012), The next Generation of Exoskeletons, *IEEE Pulse*, pp. 56-61.

Yeh IL, HolstWolf J, Elangovan N, et al. (2021), Efects of a robotaided somatosensory training on proprioception and motor function in stroke survivors, *Journal of NeuroEngineering and Rehabilitation*, **18**(1):77

Virani SS, Alonso A, Benjamin EJ, et al. (2020), Heart Disease and Stroke Statistics2020 Update: a Report from the American Heart Association, *Circulation*, **141**(9):e139-e596.

Sun J, Shen Y, and Rosen J (2021), Sensor Reduction, Estimation, and Control of an Upper-Limb Exoskeleton, *IEEE Robotics and Automation Letters*, **6**(2): 1012-1019

He C, Xiong CH, Chen ZJ, et al. (2021) Preliminary Assessment of a PosturalSynergy-Based Exoskeleton for Post-Stroke Upper Limb Rehabilitation, *IEEE Transactions On Neural Systems And Rehabilitation Engineering*, 29:1795-1805

Wang Y, Zahedi A, Zhao Y, and Zhang D (2022), Extracting Human-Exoskeleton Interaction Torque for Cable-Driven Upper-Limb Exoskeleton Equipped With Torque Sensors, *IEEE/ASME Transactions on Mechatronics*, **27**(6):4269-4280

Hayashi T, Kawamoto H, and Sankai Y (2005), Control Method of Robot Suit HAL Working as Operator's Muscle Using Biological and Dynamical Information, *IEEE International Conference on Intelligent Robots and Systems (IROS)*, **pp.**3063-3068.

Otten A, Voort C, Stienen A, *et al.* (2015), LIMPACT: A Hydraulically Powered Self-Aligning Upper Limb Exoskeleton, *IEEE/ASME Transactions on Mechatronics*, **20**(5):22852298.

Wu KY, Su YY, Yu YL, *et al.* (2019), A 5-Degrees-of-Freedom Lightweight Elbow-Wrist Exoskeleton for Forearm Fine-Motion Rehabilitation, *IEEE/ASME Transactions on Mechatronics*, **24**(6):2684 2695.

Vazzoler G; Bilancia P; Berselli G, et al. (2021), Preliminary Analysis and Design of a Passive Upper Limb Exoskeleton, International Conference on Advanced Robotics (ICAR), pp.569-574

Kapsalyamov A, Hussain S, K. Jamwal P (2020), State-of-the-Art Assistive Powered Upper Limb Exoskeletons for Elderly, *IEEE Access*, 8:178991- 179001

Rehmat N, Zuo J, Meng W *et al.* (2018), Upper Limb Rehabilitation Using Robotic Exoskeleton Systems: a Systematic Review, *International Journal of Intelligent Robotics and Applications*, **2**:283295.

Zimmermann Y, Forino A, Riener R and Hutter M (2019), ANYexo: A Versatile and Dynamic Upper-Limb Rehabilitation Robot, *IEEE Robotics and Automation Letters*, **4**(4): 3649-3656

Slucock T, A Systematic Review of Low-Cost Actuator Implementations for Lower-Limb Exoskeletons: a Technical and Financial Perspective (2022), *Journal of Intelligent and Robotic Systems*, 106(3)

Herbin P, Pajor M (2021) Human-robot cooperative control system based on serial elastic actuator bowden cable drive in ExoArm 7-DOF upper extremity exoskeleton, *Mechanism and Machine Theory*, 163(104372)

Song S, Cao Y, Wang H, et al. (2018) Adaptive Output Feedback Force Tracking Control for Lower Extremity Power-Assisted Exoskeleton, *Control Engineering and Applied Informatics*, **20**(3):60-68

Grazi L, Trigili E, Proface G, et al. (2020) Design and Experimental Evaluation of a Semi-Passive Upper-Limb Exoskeleton for Workers with Motorized Tuning of Assistance, *IEEE Transactions on Neural Systems and Rehabilitation Engineering*, **28**(10):2276-2285

Xie Q, Meng Q, Dai Y (2021), Human-robot coupling modeling and analysis for upper limb rehabilitation robots, *Technology and Health Care*, **29**(4):709-723

Winter DA (2009), Biomechanics and Motor Control of Human Movement, 4^{th} edition, *New Jersey: Jonh Wiley and Sons Inc.*

Rosen J, Perry JC, Manning N *et al.* (2005), The Human Arm Kinematics and Dynamics during Daily Activities Toward a 7 DOF Upper Limb Powered Exoskeleton, *The* 12^{th} *International Conference on Advanced Robotics-ICAR*, pp. 532-539.

Tran HT, Cheng H, Rui H, *et al.* (2016), Evaluation of a Fuzzy-based Impedance Control Strategy on a Powered Lower Exoskeleton, *International Journal of Social Robotics*, **8**:103-123.

Lee KH, Baek SG, Lee HJ, *et al.* (2018), Enhanced Transparency for Physical Human-robot Interaction using Human Hand Impedance Compensation, *IEEE/ASME Transactions on Mechatronics*, **23**(6):2662-2670.

Zeng G and Hemami A (1997), An Overview of Robot Force Control,*Robotica*, **15**(5):473-482.

Chiaverini S, Siciliano B, Villani L (1999), A Survey of Robot Interaction Control Schemes with Experimental Comparison,*IEEE/ASME Transaction on Mechatronics*, **4**(3):273285.

Tran HT, Cheng H, Duong MK, *et al.* (2014), Fuzzy-based Impedance Regulation for Control of the Coupled Human-Exoskeleton System, *IEEE International Conference on Robotics and Biomimetics*, **pp.** 986-992.

Hogan N (1985), Impedance control: An Approach to Manipulation: Part I, II, III,*Journal of Dynamic System, Measurament, and Control*, **107**(1):1-24.

Lee S and Sankai Y (2005), Virtual Impedance Adjustment in Unconstrained Motion for an Exoskeletal Robot Assisting the Lower Limb,*Advanced Robotics*, **19**(7):773-795.